MODELLING OF CURVILINEAR ELECTROSTATIC MULTIPOLES IN THE FERMILAB MUON *g*–2 STORAGE RING*

A. T. Herrod[†][1], S. Jones[1], A. Wolski[1], University of Liverpool, Liverpool, United Kingdom
I. R. Bailey[1], M. Korostelev[1], Lancaster University, Lancaster, United Kingdom
[1]also at The Cockcroft Institute, Daresbury, United Kingdom

Abstract

The Fermilab Muon *g*–2 Experiment (E989) contains flat-plate electrostatic quadrupoles, curved with the reference trajectory as defined by the constant, uniform magnetic dipole field. To understand the beam behaviour at a sufficient level, we require fast, high-accuracy particle tracking methods for this layout. Standard multipole fits to numerically-calculated 2D transverse electric field maps have provided a first approximation to the electric field within the main part of the quadrupole, but cannot model the longitudinal curvature or extended fringe fields of the electrostatic plates. Expressions for curvilinear multipoles can be fit to a 2D transverse slice taken from the central point of a numerically-calculated 3D electric field map of the quadrupole, providing a curved-multipole description. Generalised gradients can be used to model the fringe field regions. We present the results of curvilinear multipole and generalised gradient fits to the curved quadrupole fields, and the differences in tracking using these fields over 200 turns of a model of the storage ring in BMAD.

INTRODUCTION

The E989 Muon *g*–2 Experiment at Fermilab will use statically charged electrodes to focus the antimuon beam as it circulates a storage ring in a highly-uniform magnetic dipole field.

The electrodes, while flat in the transverse plane, follow the curvature of the design orbit [1]. They are positioned 50 mm from the design orbit on the vertical ($\pm y$) and horizontal ($\pm x$) sides of the vacuum chamber. The purpose is to produce a skew quadrupole field across the storage region ($\sqrt{x^2 + y^2} \leq 0.045$ m), with the horizontal defocussing counteracted by the weak focusing of the magnetic dipole. Half of the 8 quadrupoles each cover 26 degrees azimuth and the remaining half each cover 13 degrees azimuth.

The flat nature of the plates produces high-order multipole components, while the curvature with the orbit suggests that a "curvilinear multipole" expansion would be most suitable to describe the field produced.

Electrostatic plates have the feature of charge accumulation at the plate edges, thus not only do the higher-order multipoles play a significant role, but the fringe fields are also enhanced. This reduces the applicability of a multipole fringe description for the fringe fields, as it does not reproduce this phenomenon. The method of generalised

gradients [2] can model static fields which vary along the longitudinal direction.

METHOD

Bulk Field Modelling

The bulk electric field (in the region within the quadrupole where there is no longitudinal field and transverse field components have uniform values, taken here as excluding only 1 degree of azimuth at each end of each quadrupole) is modelled with a curvilinear multipole expansion [3–5] in the BMAD accelerator modelling library [6]. Two potentials can be found to satisfy the relevant Laplace equation, representing the normal and skew multipoles:

$$\phi_n^{\mathrm{re}} = -\sum_{p=0}^{\mathrm{flr}(n/2)} \frac{(iY)^{2p}}{n} \binom{n}{2p} F_{n-2p}(R)$$

$$\phi_n^{\mathrm{im}} = -\sum_{p=0}^{\mathrm{flr}(\frac{n-1}{2})} \frac{Y(iY)^{2p}}{n} \binom{n}{2p+1} F_{n-2p-1}(R)$$

where the binomial coefficient notation $\binom{n}{r}$ has been used, flr is the floor function and R and Y describe the transverse particle position in global ring (cylindrical) coordinates, normalised to the ring radius $\rho = 7.112$ m.

The functions $F_p(R)$ can be expressed as:

$$F_p(R) = \sum_{n=0}^{\mathrm{flr}(p/2)} R^{2n} \left(\alpha_{p,n} \log(R) + \beta_{p,n} \right) \tag{1}$$

with coefficients $\alpha_{p,n}$ and $\beta_{p,n}$ satisfying:

$$\alpha_{0,0} = 0, \quad \beta_{0,0} = 1; \qquad \alpha_{1,0} = 1, \quad \beta_{1,0} = 0;$$

$$\alpha_{p>1,0} = (p^2 - p) \sum_{n=1}^{\mathrm{flr}(p/2)} \frac{\alpha_{p\text{-}2,n\text{-}1} - 2n\beta_{p\text{-}2,n\text{-}1}}{4n^2},$$

$$\beta_{p>1,0} = (p^2 - p) \sum_{n=1}^{\mathrm{flr}(p/2)} \frac{\alpha_{p\text{-}2,n\text{-}1} - n\beta_{p\text{-}2,n\text{-}1}}{4n^3};$$

$$\alpha_{p>1,n>0} = (p^2 - p) \frac{\alpha_{p\text{-}2,n\text{-}1}}{4n^2},$$

$$\beta_{p>1,n>0} = (p^2 - p) \frac{n\beta_{p\text{-}2,n\text{-}1} - \alpha_{p\text{-}2,n\text{-}1}}{4n^3}.$$

The electric field is defined in terms of these as:

$$\mathbf{E} = -\sum_{n=0}^{\infty} \rho^n \left(a_n \nabla \phi_n^{\mathrm{im}} + b_n \nabla \phi_n^{\mathrm{re}} \right) \tag{2}$$

where the multipole coefficients a_n and b_n were obtained up to $n = 12$ by fitting a polynomial to E_y along the y-axis for $|y| \leq 0.048$ m, while assuming only 4-fold and skew multipole symmetries (i. e. assuming $a_n = 0 = b_{\mathrm{odd}}$).

Fringe Field Modelling

Modelling the fringe fields required fitting generalised gradients to the radial field on a cylinder centred on the design orbit (assumed straight) with $r_0 = 0.045$ m, then using the methods described in [2, 7, 8]. Due to the quadrupole geometry, the resulting field for this case can be written with only skew components without the $m = 0$ (solenoid) term.

Defined using both cylindrical and Cartesian transverse coordinates relative to the design trajectory (x, y, z and r, θ, z), the field components thus have the form:

$$E_x = \sum_{m=1}^{\infty} \sum_{l=0}^{\infty} \frac{(-1)^l m!}{2^{2l} l! (l+m)!} \Re[C_m^{[2l]}(z)] r^{2l-2+m}$$
$$\times \big((2l+m)x\cos(m\theta) + my\sin(m\theta)\big)$$

$$E_y = \sum_{m=1}^{\infty} \sum_{l=0}^{\infty} \frac{(-1)^l m!}{2^{2l} l! (l+m)!} \Re[C_m^{[2l]}(z)] r^{2l-2+m}$$
$$\times \big((2l+m)y\cos(m\theta) - mx\sin(m\theta)\big)$$

$$E_z = \sum_{m=1}^{\infty} \sum_{l=0}^{\infty} \frac{(-1)^l m!}{2^{2l} l! (l+m)!} \Re[C_m^{[2l+1]}(z)] r^{2l+m} \cos(m\theta)$$

where $C_m^{[A]} = d^A C_m / dz^A$ are the fitted generalised gradients, henceforth referred to as GGs.

Both the curvilinear multipole equations and the GG fringe fields are implemented using calculated field maps, imported to BMAD so as to be directly comparable with results from tracking through the original field data. All tracking has been done using an adaptive-step fourth-order Runge–Kutta tracking algorithm, detailed in [9].

RESULTS

The field data was produced for a plate potential of 27.2 kV [10] (resulting in a field magnitude of approximately 1 MVm^{-1} at the electrodes). The GG fit to the field data agreed within the storage region to within 20 kVm^{-1} and 500 kVm^{-1} for the transverse/longitudinal fields respectively, while the curvilinear multipole fit agreed to within 100 kVm^{-1}. Plots of the residuals of the differences between the model fields and original field data are given in Fig. 1 and Fig. 2.

A bunch of 975 on-momentum antimuons, randomly distributed in transverse phase space, was tracked around a model of the g–2 storage ring 200 times, encountering all 8 quadrupoles on each.

The tracking was done, using the same starting bunch, for cases with: the GG fringe fields with the curvilinear multipole bulk field, the GG fringe fields with the original bulk field data, the original fringe field data and curvilinear multipole bulk field, and with the original fringe field and bulk field data as a baseline. This was done so that each bunch could be directly compared with that from the baseline run.
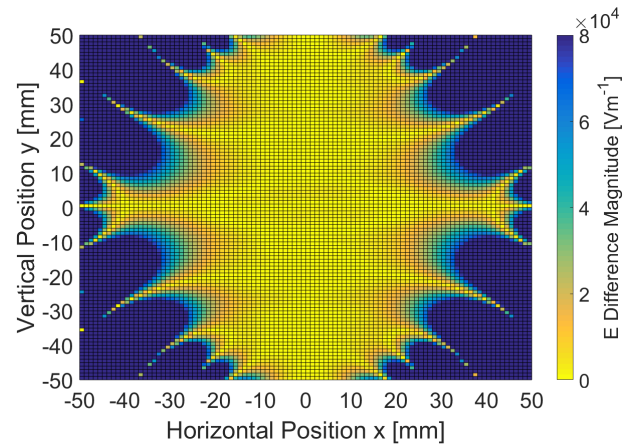
Figure 1: Magnitudes of the differences between the original field data and that reproduced from the curvilinear multipole expansion, displayed in the transverse plane.
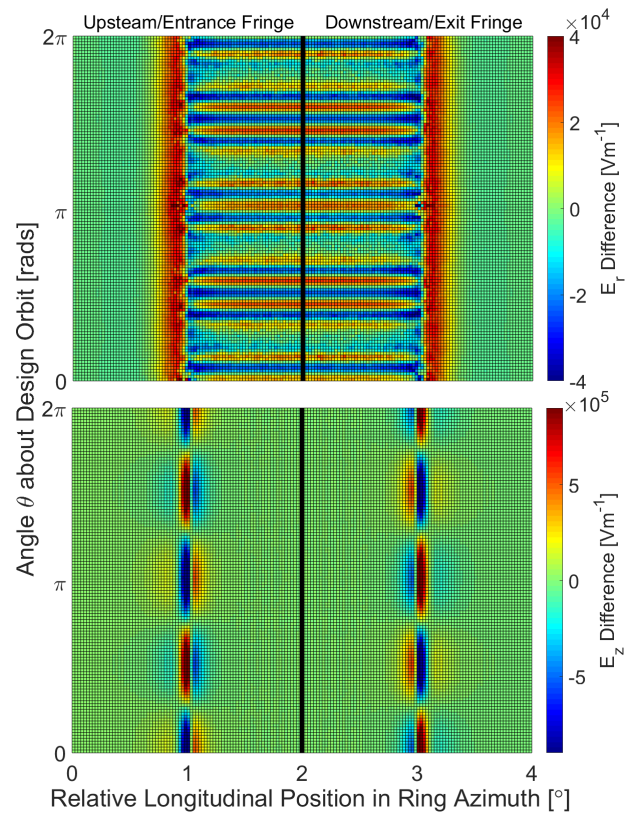
Figure 2: Differences between the original field data and that reproduced from the GGs for the radial (upper) and longitudinal (lower) components, taken on the surface of a cylinder of radius $r_0 = 0.045$ m centred on the design orbit.

To quantify these differences, the bunch emittances ϵ_x, ϵ_y and ϵ_z were calculated for each case, as were the lattice tunes and beta functions. The results for the different runs are listed in Table 1.

It was found that using the GG fringes introduced some marginal (approximately 0.2%) differences in the lattice parameters as compared to the baseline. However, using

Table 1: Lattice parameters and bunch emittances after tracking for the different cases (G for cases involving GG fringe fields and M for cases involving the curvilinear multipole bulk field).

Case	ν_x	ν_y	$\beta_x^\dagger$	$\beta_y^\dagger$	ϵ_x^*	ϵ_y^*	$\epsilon_z^\star$
Base	.9159	.4116	8.020	16.81	19.51	8.599	32.23
G	.9161	.4108	8.018	16.85	19.51	8.598	4.170
M	.9164	.4049	8.014	17.11	19.51	8.675	31.75
GM	.9165	.4039	8.013	17.15	19.54	8.680	4.186
GSt	.9167	.4036	8.011	17.17	19.40	8.605	4.201

†Units: m, *Units: mm, *Units: μm

the curvilinear multipole introduced substantially greater differences of approximately 2%.

Due to this, a further case was studied involving GG fringe fields and a straight multipole representation of the bulk field, fit to the field data using the method outlined in [11]. This fit agreed with the field data to within $6\,\mathrm{kVm^{-1}}$ within the storage region. The results for this are also displayed in Table 1 under "GSt".

The phase spaces after each run were also plotted and compared to the baseline. The transverse phase spaces overlapped very well (as could be expected by the agreement in emittance in Table 1).

However, it was found that the longitudinal phase space was substantially affected by the GG fringe fields. As suggested by the approximately 8-fold decrease in emittance, the momentum spread was reduced, as can be seen in Fig. 3. This effect was observed only for the cases using the GG fringe fields.
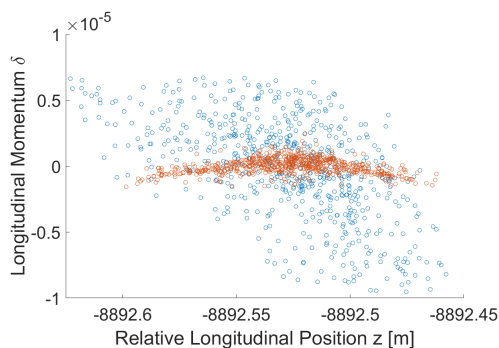
Figure 3: Longitudinal phase space after tracking for the baseline (blue) and for the GG fringes with original bulk field data (orange).

CONCLUSION

It is suggested that the inaccuracy of the curvilinear multipole fit in Fig. 1 is due to the fitting method being limited to a single axis. The improved accuracy of the straight multipole fit is not reflected in the lattice functions, where it exhibited poorer agreement with the baseline than the poorly-fit curvilinear multipole. Further research in to methods of fitting curvilinear multipoles is needed before strong conclusions can be drawn on its accuracy as a modelling method, although it has given promising results in this investigation.

The deviations in δ between tracking with and without the GG fringes is a further curiosity. This must also be investigated further, and whether the momentum of stored particles show similar behaviour in reality is unknown.

The large deviations in E_z between the GG fringe fields and the original field data appear to cancel sufficiently well, as otherwise the z coordinate of the particles would be significantly affected. The suggested cause of the difference in field from the original field data is that the fit is only performed up to $l = 2$, meaning that the longitudinal variation in the field may be being limited.

Overall, the method of fitting generalised gradients to fringe fields has been successful, as no significant deviations in tracking results have been observed as compared to the original field data. Increasing the order in m may improve transverse field agreement, however improving the fit of longitudinal field is the priority for further research, as it may also remove the apparent difference in emittance. Once satisfied with the generalised gradient representation, we can calculate the corresponding Taylor maps to reduce tracking times. With this, an in-depth investigation of the lost muon systematic [12] can be performed.

REFERENCES

[1] J. Grange *et al.*, "Muon $g-2$ Technical Design Report", `arXiv:1501.06858 [physics.ins-det]`, Jan. 2015.

[2] M. Venturini, D. Abell, and A. J. Dragt, in *Proc. ICAP'98*, pp. 184–188.

[3] P. M. McMillan, "Multipoles in cylindrical coordinates", *Nucl. Instr. Meth.*, vol. 127, pp. 471–474, 1975.

[4] S. Mane, "Solutions of Laplace's equation in two dimensions with a curved longitudinal axis", *Nucl. Instr. Meth. Phys. Res.*, sect. A 321, pp. 365, 1992.

[5] T. Zolkin, "Sector magnets or transverse electromagnetic fields in cylindrical coordinates", *Phys Rev Accel and Beams*, vol. 20, p. 043501, Apr. 2017.

[6] BMAD Accelerator Tracking Library, `https://www.classe.cornell.edu/~dcs/bmad/overview.html`

[7] M. Venturini and A. J. Dragt, "Accurate computation of transfer maps from magnetic field data", *Nucl. Instr. Meth. Phys. Res.*, sect. A 427, pp. 387, 1999.

[8] D. Newton and A. Wolski, in *Proc. PAC'09*, pp. 3943–3945.

[9] *BMAD Manual*, D. C. Sagan, Cornell University, NY, USA, Apr. 2017, pp. 144–145; `https://www.classe.cornell.edu/~dcs/bmad/manual.html`

[10] W. Wu, private communication, Nov. 2016.

[11] A. Wolski, *Beam Dynamics in High Energy Particle Accelerators*. London, UK: Imperial College Press, 2014.

[12] S. Ganguly *et al.*, "Lost muon study for the muon $g-2$ experiment at Fermilab", presented at IPAC'17, Copenhagen, Denmark, May 2017, paper WEPIK119.